

Investigation into potential TEC changes due to 9 seismic tremors of 2021–2022

Kunvar S. YADAV* , Rakesh B. VADNATHANI ,
Mangesh D. BHOYA , Keyurgiri R. GOSWAMI 

Department of Physics, Faculty of Sciences, Mehsana Urban Institute of Science (MUIS),
Ganpat University, Kherva, Mehsana, Gujarat, India;
e-mails: kunvar.yadav@gmail.com, vадnathanirakesh165@gmail.com,
mangeshbhoya@gmail.com, keyurgiri562000@gmail.com

Abstract: This research document delves into the analysis of alterations in Total Electron Content (TEC) as identified through GPS observations leading up to nine earthquakes that transpired between the late months of 2021 and 2022. The comprehensive study investigates the TEC variations and provides a detailed examination of heat maps centred around the earthquake epicentres. These heat maps, characterized by diverse latitudes and longitudes, play a pivotal role in validating the precise locations of the earthquake epicentres. Notably, the examination of these maps unveils discernible GPS TEC variations several days before the occurrence of each earthquake. In addition to the TEC analysis, the research sheds light on the fluctuations in solar magnetic parameters. The study elucidates instances where TEC peaks surpassed normal values, particularly during periods characterized by minimal solar radiation effects. This correlation between solar magnetic parameters and TEC fluctuations adds a nuanced layer to the understanding of the complex interplay of factors leading to seismic events. The cumulative findings derived from the investigation point towards a compelling conclusion: GPS TEC observations and the analysis of heat maps serve as indispensable indicators for identifying precursory signs that precede an impending earthquake. This multidimensional approach enhances our comprehension of the temporal and spatial aspects of seismic activity and underscores the potential significance of solar magnetic parameters in influencing such geophysical events.

Key words: earthquake, TEC (total electron content), STEC (slant total electron content), VTEC (vertical total electron content), percentage VTEC, solar flux F10.7, Dst (disturbance storm time index), Ap (geomagnetic index), heat maps

1. Introduction

An earthquake is a natural phenomenon that occurs frequently. The purpose of them is to release energy from the earth, which was accumulated

*corresponding author, e-mail: kunvar.yadav@gmail.com

under the lithosphere (earth's uppermost layer). If an earthquake is of a large magnitude and takes place near extensively developed infrastructure and high populations, it causes a lot of damage. Every year, earthquakes lead to the deaths of thousands of people all over the world. Therefore, they are a subject worth studying and predicting (*Rikitake, 1968*). Recent decades have seen the introduction of many different methods, such as TEC (total electron content) enhancements (*Agayeva, 2012*), radon gas emission, troposphere temperature increase, and humidity changing in the earthquake preparatory zone (*Pulinets et al., 2006*), electromagnetic fields, surface air temperature and sea surface temperature (*Ghamry et al., 2021*), surface latent heat flux, chlorophyll and upwelling flux enhancement before the earthquake (*Singh et al., 2006*). An investigation of TEC anomalies prior to earthquakes is presented in this paper.

TEC is one of the most important components of the ionosphere. It is well known that the ionosphere is composed of charged particles, including electrons (*Duncan, 1960*). The ionosphere is a global electric circuit. Several factors affect TEC, including solar radiation (*Yadav et al., 2016a*), thunderstorms, lightning, volcanic activity, and seismic activity (*Yadav and Pathak, 2018; Yadav et al., 2016b; He et al., 2012; Zhu and Jiang, 2020*). *Sharma et al. (2017)* in their work showed that variations of vertical total electron content were seen in the Himalayan region for all 4 earthquakes, these variations were seen increasing as they moved closer to the epicentre of the earthquake using ground-based GNSS data. In the year 2022, *Asaly et al. (2022)* performed a support vector machine (SVM) technique to predict the precursors in the ionosphere prior to the seismic events; they were able to predict true positive results with 80% accuracy and true negative results with 85.7% accuracy. *Ghimire and Chapagain (2022)* used 6 GPS receivers' data to analyse the TEC disturbances due to the 7.8 magnitude Nepal earthquake of 25th April, 2015. GPS transmission frequencies are delayed when TEC is disturbed because the ionosphere functions as a dispersive medium. It is possible to measure TEC values in the atmosphere based on these delays and pseudo-ranges of these frequencies. In addition to monitoring the ionosphere, GPS also provides a real-time picture of the whole atmosphere. To make GPS work, 24 satellites are dispersed across six orbital planes across the planet. Each satellite transmits two frequencies of signals $f_1 = 1575.42$ MHz and $f_2 = 1227.60$ MHz the total number

of electrons is known as the total electron content or TEC, inside 1 m^2 of cross-section; 1 TEC unit is equal to 10^{16} el./m^2 . Such studies of TEC prior to an earthquake data were conducted before for many earthquake cases (*Liu et al., 2004; Afraimovich and Astafyeva, 2008; Klimenko, et al., 2011*) also showed that, 3 days before the strong Wenchuan earthquake on May 9, 2008, TEC enhancements above the earthquake preparation area and magneto-conjugated area were also observed.

There are a few reasons that are responsible for the enhancement in TEC, like radon gas emission, atmospheric gravity waves (AGW), and piezoelectric effects cause seismogenic vertical electric fields which have been studied by *Namgaladze et al. (2009)* in which the positive and negative electric charges need to be located at the western and eastern boundaries of the region respectively. The efficiency of the suggested mechanism was investigated through the simulation of the ionospheric reaction to the electric field produced by the specified charge arrangement. *Akhoondzadeh (2012)* also showed TEC anomalies of the Tohoku earthquake of 2011. *Tariq et al. (2019)* showed anomalous VTEC within 10 days before an earthquake for 7+ magnitude earthquakes in Asian countries during 2015–2017 in low solar activity period. The result section introduces TEC plotting with heat maps (latitude and longitude) to show the relationship between the TEC coordinates and the earthquake preparatory zone area. Earthquakes that



Fig. 1. Displays the closest IGS stations and the epicentre of each of the ten earthquakes (the IGS stations are denoted by black dots and earthquake epicentres are denoted by red dots).

occurred throughout the world in the late months of 2021 and 2022 are shown in Fig. 1. TEC variations in the ionosphere are not too far from the epicentres of earthquakes as shown in Fig. 1 by IGS (International GNSS (Global Navigation and Satellite System) service) stations (black dots) and earthquakes (red dots).

2. Data and analysis

Earthquake data (epicentre location, magnitude, pre-shock, and aftershock details) were obtained from the USGS (United States Geological Survey) website (<https://earthquake.usgs.gov/>). In Table 1, we present seismic data from 9 earthquakes in the late months of 2021 and 2022 (earthquake location, date, time, and the location of the IGS station). Since for other earthquake cases of 2021–2022, we couldn't find the GPS receiver data, hence only a few earthquake data have been displayed here of magnitude 6 and higher. NASA's website (<https://cddis.nasa.gov/>) was used to collect data on satellites corresponding to these earthquake regions.

STEC and VTEC formulations containing L1 and L2 carrier phase frequencies and pseudo ranges of L1 and L2 were also used. P1 (code C/A pseudo-range, of L1 frequency), P2 (pseudo-range P-code, in meter, of L2 frequency), L1 (carrier phase, in cycles, on L1 frequency), and L2 (carrier phase, in cycles, on L2 frequency) with a time resolution of 30 s are all included in the RINEX data obtained from GPS receivers. From an IGS data collection in RINEX format, the STEC (slant total electron content) was calculated by:

$$STEC = \left(\frac{f_1^2 f_2^2}{f_1^2 - f_2^2} \right) \left(\frac{P_1 - P_2}{40.3} \right),$$

where f_1 (1227.60 MHz) and f_2 (1575.42 MHz) are current GPS broadcast frequencies. Using an appropriate mapping function of distinct ionosphere pierce point (IPP) location, STEC was transformed to VTEC, the mapping function $S(E)$ is defined as:

$$S(E) = \frac{1}{\cos \chi'}, \quad VTEC = \frac{STEC}{S(E)},$$

where:

Table 1. Data and time of all 9 earthquakes (late 2021 – 2022).

Sr. No.	Location of earthquake	Date	Time (UT)	IGS stations
1	Mid-Indian Ridge (9°11' S, 67°16' E) M 6.0	2 nd Oct. 2021	20:43	DGAR (7°16' S, 72°22' E)
2	Chile (28°44' S, 71°29' W) M 6.0	4 th July 2021	01:29	SANT (33°9' S, 70°40' W)
3	California (38°30' N, 119°30' W) M 6.0	8 th July 2021	22:49	BILL (33°35' N, 117°4' W)
4	Nicaragua (11°13' N, 86°32' W) M 6.3	9 th Nov. 2021	06:25	SSIA (13°42' N, 89°32' W)
5	Haiti (18°26' N, 73°29' W) M 7.2	14 th Aug. 2021	12:29	RDSO (18°28' N, 69°55' W)
6	Peru (4°59' S, 80°37' W) M 6.2	30 th July 2021	17:10	RIOP (1°39' S, 78°39' W)
7	Fiji region (20°7' S, 178°21' W) M 7.0	12 th Nov. 2022	07:09	TONG (21°9' S, 175°11' W)
8	Solomon Islands (9°49' S, 159°28' E) M 6.0	22 nd Nov. 2022	02:38	SOLO (9°26' S, 159°57' E)
9	Samoa Islands region (15°21' S, 172°69' W) M 6.8	4 th Dec. 2022	19:24	TONG (21°9' S, 175°11' W)

$$\text{PERCENTAGE VTEC (\%)} = \frac{VTEC}{UPPER LIMIT} \times 100,$$

$$\cos \chi' = \sqrt{1 - \left(\frac{R_x \cos \chi^2}{R_x + h_m} \right)^2}$$

R_x = Earth mean radius, 6371 km, χ = angle of elevation, χ' is zenith angle, and, h_m = 350 km (IPP), is the ionospheric shell's height above the earth's surface (Rama Rao et al., 2006).

We compute the median X of the 60 days prior earthquake date and the VTEC value in the Y median in this study to discover an abnormality in ionospheric TEC. As a result of calculating the interquartile range based on the VTEC data, the upper limit is derived.

In order to extract TEC text files from CDDIS (Crustal dynamics data information system) website via satellite, a GPS Rinex algorithm developed by Dr. Gopi Krishna Seemala (*Seemala, 2011*). Text files were converted into 60 days of 24-hour data with LabVIEW coding. These data sets were used to plot Percentage VTEC v/s Days and Heat maps. Solar indices are plotted here as well, to show disturbances in the magnetic field and electric field of earth. The results shown here were produced using Tableau. Using NASA's OmniWeb website (<http://omniweb.gsfc.nasa.gov/form/dx1.html>), solar flux F10.7, disturbance storm time index (Dst), and geomagnetic index Kp were obtained. A few more parameters about solar radiation and disturbances caused by solar radiation can be found on this site.

3. Results

VTEC values for each hour for the 30 days prior to and following an earthquake are displayed in graphs of percentage VTEC% v/s Day. In VTEC, heat maps on a global basis are also displayed here. These maps show where VTEC is located on a global scale. Using VTEC values, an upper was discovered in order to determine which VTEC results would be regarded as anomalous.

Figure 2a, which depicts the magnitude 6 Mid-Indian range earthquake, provides indications that the VTEC is increasing over the upper limit (100% is the upper limit border, which is indicative of the quartile range taken into account from the VTEC data). On days 25, 23, and 8 to 3 prior to the earthquake, the VTEC began to exceed the upper limit. The gap between the anomalies started to close as the earthquake day (2nd October 2021) drew near. There were certain days when the VTEC crossed the 150% mark, which means the VTEC readings were greater than 1.5 times the upper limit value. Solar indices graphs (about 30 days before and after the earthquake date) are shown in Fig. 2b. It's clearly visible that $F10.7 < 120$ sfu and $Dst < -50$ nT. Nonetheless, VTEC levels exceed the established upper limit. Even after the earthquake, there remain significant variances in TEC.

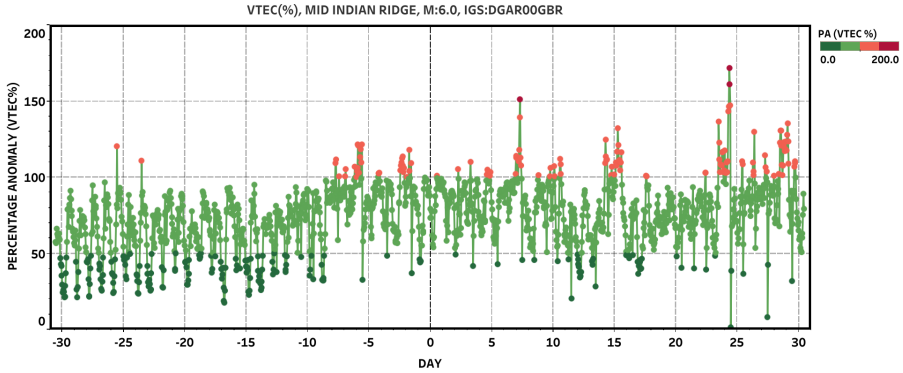


Fig. 2a. Shows percentage VTEC (%) v/s Day (green values indicate low VTEC%, orange and red values indicate high VTEC%). As the earthquake day approaches, the TEC value is rising, as can be seen. VTEC values above 100% are considered abnormal fluctuations. IGS station is DGAR00GBR station from the United Kingdom.

Given that the earthquake made the lithosphere less restrictive to constrain the seismic energy, these variations may be the energy that escapes from the lithosphere.

On a world map scale, Figure 2c displays the VTEC% anomalies associated with the Mid Indian Range Earthquake. It is clear that anomalies were reported all around the earthquake’s epicentre.

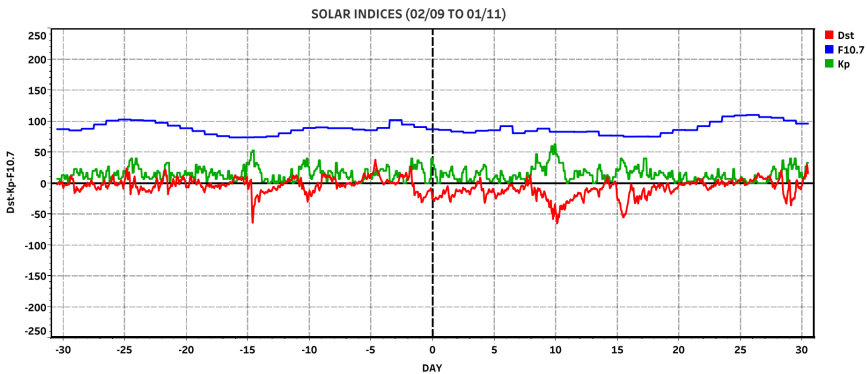


Fig. 2b. Displays values for F10.7, Dst, and Kp that are insufficient to justify such TEC abnormalities. Disturbance caused by solar radiation is seen 15 days before the earthquake. But the electron density was observed low during this time period. After the earthquake %VTEC showed a spike going above 150% but the solar radiation effects were not that effective.

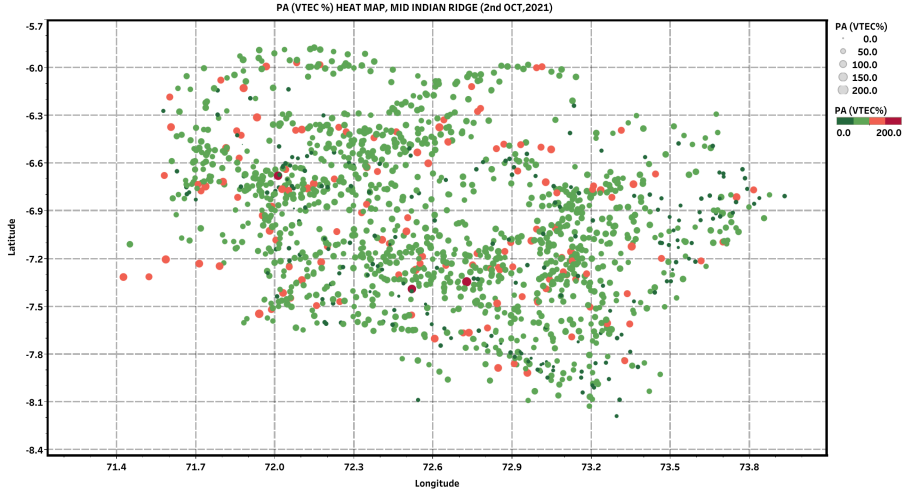


Fig. 2c. Heat map is displayed nearby Mid Indian range on a global scale. Red and orange dots indicate VTEC% abnormalities (scattered over a large region). The coordinates of the earthquake epicentre is $9^{\circ}11' S$, $67^{\circ}16' W$, which is not very far from the recorded VTEC% values.

In contrast to the first result, in the second case (Fig. 3a), VTEC% anomalies were seen almost daily leading up to the earthquake (4th July 2021, M 6.0), in the Mid Indian range ocean. Since solar radiation is very low ($F_{10.7} < 120$ sfu and $Dst < -80$ nT). According to Figure 3b, which shows the period from 4 June to 3 August, this VTEC% cannot be attributed to solar radiation but rather to seismic activity. This is also true in this instance. VTEC anomalies following an earthquake are seen.

Near Santiago, which is almost 400 km from the earthquake's epicentre, Figure 3c depicts VTEC% anomalies as a heat map on a global scale. It is clear that anomalies were reported all around the epicentre of the earthquake. These findings resemble those of the mid Indian range earthquake despite a distance of about 500 km between the earthquake's epicentre and the satellite VTEC data.

Figure 4a displays the California earthquake's VTEC% data (8th July 2021, M 6.0). The figure clearly illustrates variations in VTEC% above the pre-set upper limit (100%), as can be seen. VTEC varies continuously from 6 to 17 days, from 25 to 30 days, and 2 to 3 days prior to the earthquake. Additionally, there are post-earthquake anomalies. Around the 25th day fol-

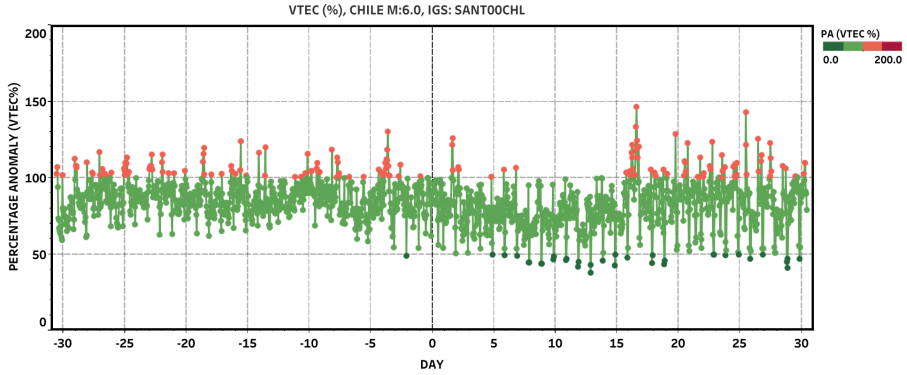


Fig. 3a. Shows percentage VTEC (%) v/s Day (green values indicate low VTEC%, orange and red values indicate high VTEC%). As the earthquake day approaches, the TEC value is rising, as can be seen. VTEC values above 100% are considered abnormal fluctuations. IGS station is SANT00CHL from Chile.

lowing the earthquake, VTEC crossed the 150% line, meaning VTEC was 1.5 times higher than the upper limit.

The data of solar flux, solar indices, and earth’s electric field disturbances are displayed in Fig. 4b. Both 30 days before and 30 days after the earthquake, the solar weather was normal. The region over which these anomalies are reported near Los Angeles (about 400 km from the earthquake’s epicentre) is depicted in Figure 4c’s heat map representation of the VTEC% of

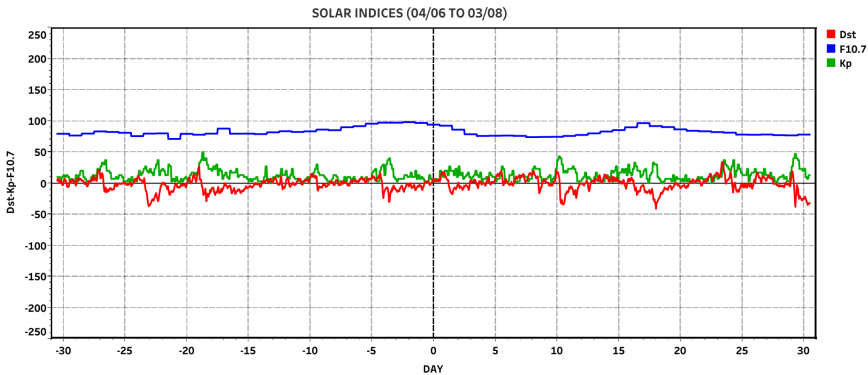


Fig. 3b. Displays values for F10.7, Dst, and Kp that are insufficient to justify such TEC abnormalities. The solar indices show no irregular variations that can affect the electron density of the ionosphere at a scale where VTEC% values above 100% were spotted every day before the earthquake day.

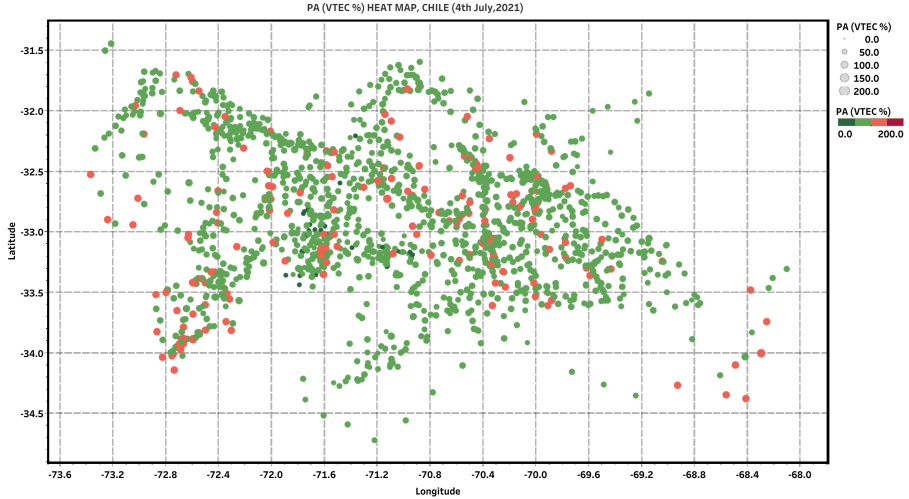


Fig. 3c. Heat map is displayed around Santiago (about 400 km from the epicentre) on a global map scale. Red and orange dots indicate VTEC% abnormalities (scattered over a large region). The coordinate of the earthquake epicentre is shown in Table 1 ($28^{\circ}44' S$, $71^{\circ}29' W$), which is in the region of recorded VTEC% values.

the California earthquake (8th July, 2021). These outcomes correspond to the case of the Chile earthquake (Fig. 3c).

Figure 5a (see the online Supplement) displays the earthquake’s VTEC%

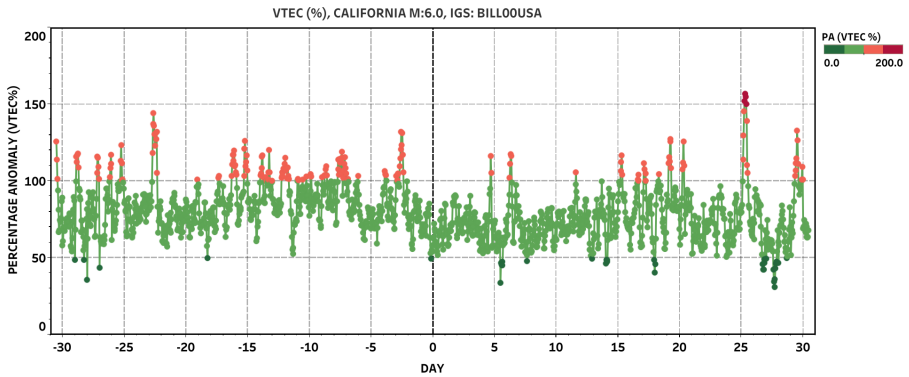


Fig. 4a. Shows percentage VTEC (%) v/s Day (green values indicate low VTEC%, orange and red values indicate high VTEC%). As the earthquake day approaches, the TEC value is rising, as can be seen. VTEC values above 100% are considered abnormal fluctuations. IGS station is BILL00USA from Chile.

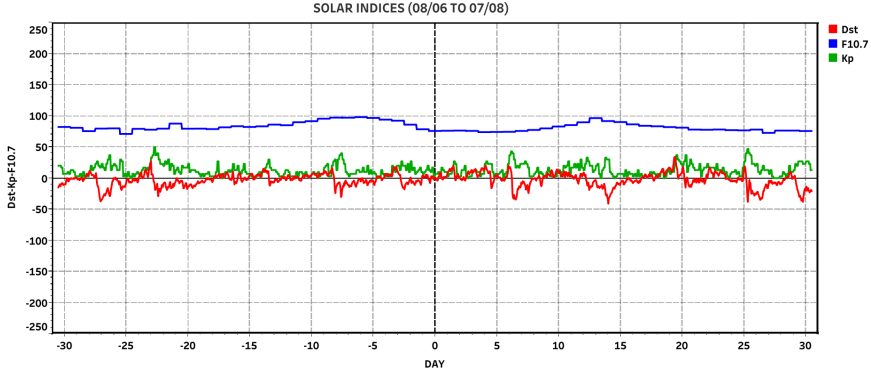


Fig. 4b. Displays values for F10.7, Dst, and Kp that are insufficient to justify such TEC abnormalities. The solar indices show no irregular variations that can affect the electron density of the ionosphere at a scale where VTEC% values above 100% were spotted every day before earthquake day.

in Nicaragua (9th November 2021, M 6.3). 30 days prior to the earthquake, VTEC anomalies were seen crossing the 150% threshold and space weather conditions were quiet. However, Dst disturbances above -80 nT were seen

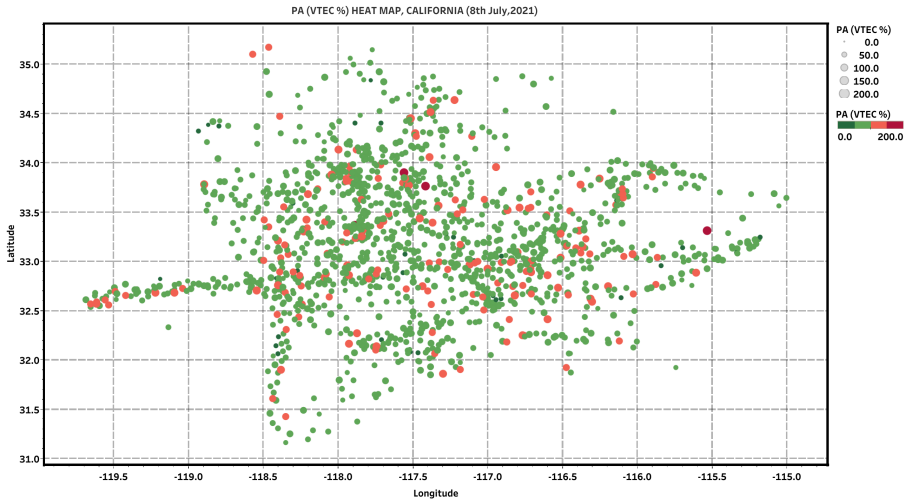


Fig. 4c. Heat map near Los Angeles is displayed on a global map (400 km from the earthquake’s epicentre). Red and orange dots indicate VTEC% abnormalities (scattered over a large region). The coordinate of the earthquake epicentre is shown in Table 1 ($38^{\circ}30' N, 119^{\circ}30' W$), which is near the region of recorded VTEC% values.

5 to 7 days prior to the earthquake, as shown in Fig. 5b (in Supplement). Thus, there is a chance that VTEC anomalies may result from that. Anomalies following the earthquake were seen in this instance as well.

Wang et al. (2008) demonstrated comparable findings of brief TEC enhancements in the equatorial zone, with correlations between TE and Dst displaying a rising trend from morning to afternoon, even amidst periods of low geomagnetic activity.

Figure 5c (in Supplement) depicts the case study for the Nicaragua earthquake (9th November 2021), in which anomalies in the VTEC% were seen over El Salvador (approximately 400 km from the epicentre of the earthquake). In all the cases of this study, such long-range VTEC anomalies were seen. This makes it abundantly clear that seismic activities have a very wide-ranging impact on the ionosphere.

Figure 6a (in Supplement) displays the Haiti earthquake's VTEC% data (14th August 2021, M 7.2). On the 28th day prior to the earthquake is when VTEC anomalies were seen to be their highest, and this is also the time when solar flux and Dst values were seen to be at their lowest (Fig. 6b, in Supplement), which indicates that there was no solar activity during this time. Continuous VTEC% anomalies were seen 10 to 25 days prior to the earthquake. Electric field disturbances peaked after the earthquake, which suggests bizarre solar activity. When compared to the number of anomalies seen in the other five cases shown above, the VTEC% anomalies in the Peru earthquake case with a magnitude of 6.2 (Fig. 7a, in Supplement) were quite normal. Solar radiation was the cause of the VTEC being almost 200% after the earthquake on the 28th day (high Dst on the same day in Fig. 7b, in Supplement).

In the M 7.0 Fiji island earthquake case (Fig. 8a, in Supplement), VTEC% anomalies were seen for quite a few days (9th November 2022) before the earthquake, and there were continuous variations. Around -80 nT of Dst was measured for about half of the VTEC anomalies (Fig. 8b, in Supplement). The beginning of solar cycle 25 in mid-2022 resulted in a significant increase in the number of solar radiation effects on the earth's magnetic field. Following the earthquake, 8 VTEC anomalies were observed above 150%, none of which occurred during the period when Dst and F10.7 were high. It was evident from heat maps on a global scale that all these VTEC% variations for the Fiji case were located very close to the area where the

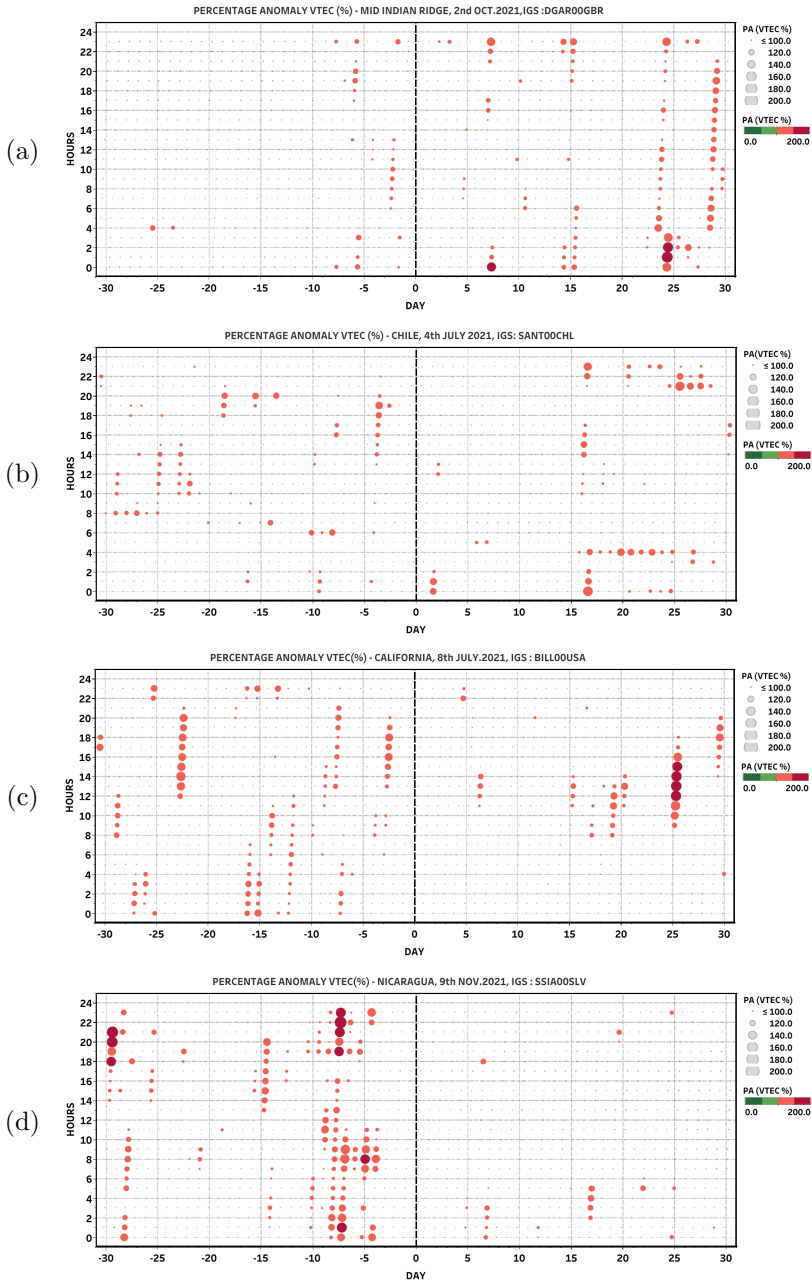
earthquake's epicentre was reported. While abnormal VTEC (orange and red) range from 100–200%, green dots show VTEC from 0–99% (dark green dots range from 0–49%, light green dots range from 50–99%).

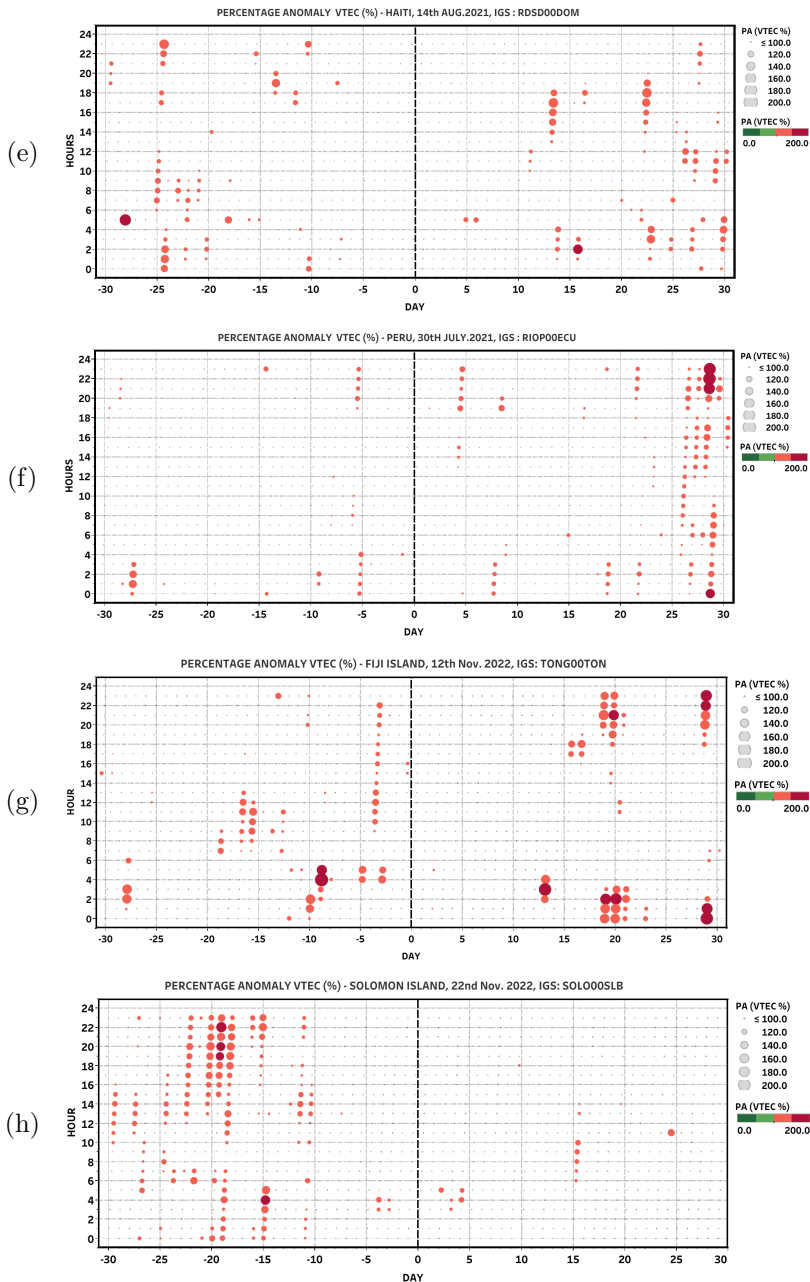
The Solomon Island case showed similar outcomes as well (M 7.0, 22nd October, 2022). Before the earthquake, VTEC anomalies were seen frequently (Dst was seen to be a little higher for a few days). However, solar flux (F10.7) was nearly 150 sfu in the Fig. 9b (in Supplement), despite the fact that no abnormal changes in VTEC were observed. These kinds of occurrences raise numerous concerns regarding the ionosphere's vulnerability to solar radiation. These VTEC% anomalies (Fig. 9c, in Supplement) were unquestionably in the earthquake epicentre region, according to heat maps results. For the Samoa Island earthquake case (M 6.8), similar conclusions were also attained. Right before the earthquake day (4th December 2022), VTEC% anomalies were seen to spike, and Dst readings were very low at that time (Fig. 10b, in Supplement). The heat map results also revealed VTEC variations very near the epicentre.

Directly above the earthquake's epicentres, this kind of TEC enhancement was seen at all IGS stations. These variations were detected by some satellites up to 8–9° latitude and longitude away from the earthquake's epicentre. According to Chakravarty's research, TEC variations can occur up to 13° latitude (*Chakravarty, 2014*). Given the large number of anomalies that were noticed both before and after each earthquake, it is crucial to provide additional proof in the results that these anomalies were not just noticed at noon time in each of these regions. Which makes the Hour v/s Days results very instructive (Fig. 11a-i shows that high anomalies were observed during night-time and evening as well). These findings demonstrate the onset of VTEC's growth, its peak, and the beginning of its decline. Researchers have previously studied night-time VTEC anomalies in Bhopal, India (*Jain et al., 2011*). Figure 11c, however, revealed that night-time TEC enhancements were ascertained in California (38° N latitude earthquake case).

4. Discussion

This paper talks about 9 earthquakes, and TEC anomalies reported prior to these earthquakes. Such results of previous earthquakes were also shown by





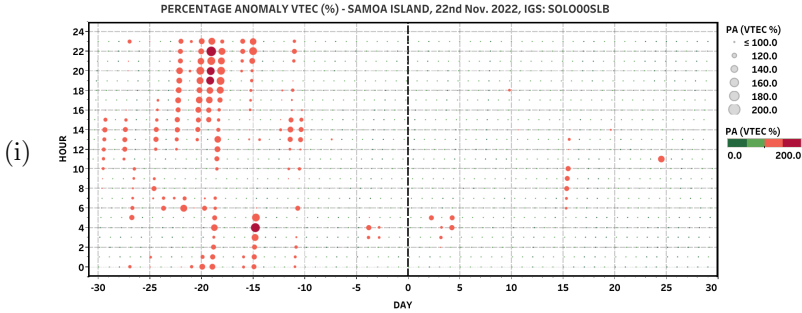


Fig. 11a-i. Abnormal VTEC% is displayed for each of the 24 hours of the day for all earthquakes (higher VTEC% values are indicated by orange and red dots that are sized larger than normal VTEC%). Note: These variations are not direct VTEC values but the percentage VTEC, which shows that the VTEC values are not going above upper limit decided for the particular cases VTEC values, and these values are nullified with small dots shown in map. Values of VTEC going above upper limit are shown with bigger dots (the size of the dots are in positive correlation with the VTEC).

Liu et al. (2010) and *Yadav et al. (2023)*, by contour plots (*Devi et al., 2004*; *Karia and Pathak, 2011*; *Shah and Jin, 2015*; *Başçiftçi and Bülbül, 2022*; *Eisenbeis and Occhipinti, 2021*; *Ulukavak et al., 2020*), later in 2022 *Liu et al. (2023)* showed TEC anomalies with two more additional parameters (ions temperature and ions velocities) of 2 Iran-Iraq border earthquakes of 2017. There are many theories present in the scientific community which talk about the relationship between seismic activity and Ionospheric TEC anomalies prior, during and after the earthquakes. One of these theories is, the direct wave propagated by the compression of rocks near the epicentre is likely to be affected by piezoelectric and turboelectric effects. At the earth's surface, rock-induced stress manifests as an electric charge and an electric current in the atmosphere and ionosphere (*Freund, 2007*; *Uyeda et al., 2009*), later in 2021 *Freund et al. (2021)* showed detailed physical processes involved in the enhancement of electron and ion density. The electron concentration in height is altered or redistributed by electric current in the ionosphere and joule heating. There have been reports of gases escaping into the atmosphere after being heated by underground liquids rising (*Troyan and Hayakawa, 2002*). The primary source of upward energy fluxes caused by atmospheric gravity waves (AGWs) was gas water released from the preparatory earthquake zone, according to *Molchanov*

and Hayakawa (2008). It is believed that AGW waves are moulding natural ionospheric turbulence (Liperovsky et al., 2000; Molchanov et al., 2004). It is likely that the pre-seismic perpendicular Electric field on the earth's surface, which causes disruption over the F-region ionosphere, resulted in an electric field that is parallel to the geomagnetic field line. The F-region will pre-start spreading along conducting magnetic field lines and cover a larger area when it is disturbed in that area (Liu et al., 2006).

There are also theories given by *Pulinets and Ouzounov (2011)* on LIAC coupling mechanism: (1) the precursory signature of lower and upper atmosphere anomalies discovered seven to one days before a seismic event near the epicentre is lithosphere radiation (radon in the vicinity of active tectonic faults). (2) When a particle decays, it creates air ionization, which triggers a chain reaction involving all layers of the atmosphere. During ionization, a great deal of thermal energy is released under the surface of the crust, which allows water molecules to run free when attached to the ions they produce. (3) Surface latent heat and unusual heat-energy fluxes, as shown by remote sensing satellites, have been observed as heating effects in the sequential chain with some delay from lower to higher atmosphere. (4) Variations in the lithosphere-ionosphere electrical circuit parameters are produced locally by variations in tropospheric air phenomena over the earthquake-preparation zone. (5) As air ascends due to the release of latent heat, various ion cluster nuclei ascend to high altitudes, forming clouds. Due to this process, a force field directed upward is observed over the seismically active area. (6) Electricity anomalies in the atmosphere influence ion temperatures, ion concentrations, and electron densities. (7) Contributory electrons alter the D-region of the ionosphere, causing VLF waves to propagate abnormally among the waveguide Earth-ionosphere. (8) In the planned lay idea, the scientific justification for a coordinated observation and validation of earthquake precursors is laid out.

5. Conclusion

Nine earthquake cases from the final months of 2021 and 2022 are discussed in this paper. Additionally, it discussed the TEC anomalies that were detected 30 days prior to 30 days following all earthquakes and were reported within 500 km of the epicentre. In all cases, these maps displayed anomalous

variations. Solar indices demonstrated that, at least for earthquake cases in 2021, solar conditions were calm. In the final three cases of this study, solar indices confirmed that the effects of the 25th solar cycle began to manifest as early as 2022, which caused Dst and Kp values to spike above their normal levels. All of these variations were found to be very close to the earthquake's epicentre, according to VTEC% heat maps on world map. Even though there were some days when VTEC spiked, the geomagnetic condition was calm. There were night-time TEC enhancements recorded in all of these cases, and since solar radiation is at its lowest during the night, as seen in the previous results, we can speculate that these anomalies are caused by seismic activity. However, some studies hypothesised that the neutral wind, electrodynamic E-B drift, and post-sunset increase in the equatorial fountain were the root causes of the night-time enhancement in TEC. Therefore, it is difficult to determine what factors are causing TEC to soar at night. If all effects are considered together, finding a way to distinguish between disturbances brought on by each effect will need to be researched. There are some disadvantages to this method. For instance, because TEC is high in the summer, it can be difficult to separate the portion of the TEC increase brought on by seismic activity from the portion brought on by the radiation effect.

Acknowledgements. I am deeply grateful for the invaluable support and inspiration provided by numerous individuals throughout my journey. Their guidance and encouragement have been instrumental in my success. Their influence is evident in every aspect of my work, and I am forever indebted to them. I extend my heartfelt thanks to my mentor, Dr. Kunvar S. Yadav, Assistant Professor in the Department of Physics, whose guidance has been invaluable. I am also grateful to Dr. Darshan B. Desai, Head of the Department of Physics at Mehsana Urban Institute of Sciences, for his support. I am thankful to Dr. S. S. Pancholi, Executive Dean of the Faculty of Sciences at Ganpat University, and Dr. Amit K. Parikh, Dean of the Faculty of Sciences at Ganpat University and Principal of Mehsana Urban Institute of Sciences, for providing me with the necessary resources for my research. I express my sincere gratitude to all the members of the Physics Department at Mehsana Urban Institute of Sciences for their assistance at every stage of my work. Lastly, I am deeply appreciative of my loving family for their unwavering support and blessings. I dedicate my research work to them, as their encouragement and vision have been indispensable to my achievements.

References

- Afraimovich E. L., Astafyeva E. I., 2008: TEC anomalies—Local TEC changes prior to earthquakes or TEC response to solar and geomagnetic activity changes? *Earth Planets Space*, **60**, 9, 961–966, doi: 10.1186/BF03352851.
- Agayeva L. A., 2012: Major factors, defining seismic hazard of Turkmenistan. In: Otajanov D., Usmanova M.: Proceedings of the international conference on “Complexity in earthquake dynamics: From nonlinearity to earthquake prediction and seismic stability”, January 25–26, 2012, Tashkent, Uzbekistan, 83–88.
- Akhoondzadeh M., 2012: Anomalous TEC variations associated with the powerful Tohoku earthquake of 11 March 2011. *Nat. Hazards Earth Syst. Sci.*, **12**, 5, 1453–1462, doi: 10.5194/nhess-12-1453-2012.
- Asaly S., Gottlieb L.-A., Inbar N., Yuval Reuveni Y., 2022: Using support vector machine (SVM) with GPS ionospheric TEC estimations to potentially predict earthquake events. *Remote Sens.*, **14**, 12, 2822, doi: 10.3390/rs14122822.
- Başçiftçi F., Bülbül S., 2022: Investigation of ionospheric TEC changes potentially related to Seferihisar-Izmir earthquake (30 October 2020, MW 6.6). *Bull. Geophys. Oceanogr.*, **63**, 3, 403–426, doi: 10.4430/bgo00394.
- Chakravarty S. C., 2014: A novel approach to study regional ionospheric variations using a real-time TEC model. *Positioning*, **5**, 1, 42518, doi: 10.4236/pos.2014.51001.
- Devi M., Barbara A. K., Depueva A., 2004: Association of total electron content (TEC) and f_oF2 variations with earthquake events at the anomaly crest region. *Ann. Geophys.*, **47**, 1, 83–91, doi: 10.4401/ag-3261.
- Duncan R. A., 1960: The equatorial F -region of the ionosphere. *J. Atmos. Terr. Phys.*, **18**, 2-3, 89–100, doi: 10.1016/0021-9169(60)90081-7.
- Eisenbeis J., Occhipinti G., 2021: The TEC enhancement before seismic events is an artifact. *J. Geophys. Res. Space Phys.*, **126**, 4, e2020JA028733, doi: 10.1029/2020JA028733.
- Freund F. T., 2007: Pre-earthquake signals – Part II: Flow of battery currents in the crust. *Nat. Hazards Earth Syst. Sci.*, **7**, 5, 543–548, doi: 10.5194/nhess-7-543-2007.
- Freund F., Ouillon G., Scoville J., Sornette D., 2021: Earthquake precursors in the light of peroxy defects theory: Critical review of systematic observations. *Eur. Phys. J. Spec. Top.*, **230**, 1, 7–46, doi: 10.1140/epjst/e2020-000243-x.
- Ghamry E., Mohamed E. K., Abdalzaher M. S., Elwekeil M., Marchetti D., De Santis A., Hegy M., Yoshikawa A., Fathy A., 2021: Integrating pre-earthquake signatures from different precursor tools. *IEEE Access*, **9**, 33268–33283, doi: 10.1109/access.2021.3060348.
- Ghimire B. D., Chapagain N. P., 2022: Ionospheric anomalies due to Nepal earthquake-2015 as observed from GPS-TEC data. *Geomagn. Aeron.*, **62**, 460–473, doi: 10.1134/S0016793222040041.
- He L., Wu L., Pulnests S., Liu S., Yang F., 2012: A nonlinear background removal method for seismo-ionospheric anomaly analysis under a complex solar activity scenario: A case study of the M9.0 Tohoku earthquake. *Adv. Space Res.*, **50**, 2, 211–220, doi: 10.1016/j.asr.2012.04.001.

- Jain A., Tiwari S., Jain S., Gwal A. K., 2011: Nighttime enhancements in TEC near the crest of northern equatorial ionization anomaly during low solar activity period. *Indian J. Phys.*, **85**, 1367–1380, doi: 10.1007/s12648-011-0159-7.
- Karia S. P., Pathak K. N., 2011: GPS based TEC measurements for a period August 2008–December 2009 near the northern crest of Indian equatorial ionospheric anomaly region. *J. Earth Syst. Sci.*, **120**, 851–858, doi: 10.1007/s12040-011-0114-1.
- Klimenko M. V., Klimenko V. V., Zakharenkova I. E., Pulnits S. A., Zhao B., Tsidilina M. N., 2011: Formation mechanism of great positive TEC disturbances prior to Wenchuan earthquake on May 12, 2008. *Adv. Space Res.*, **48**, 3, 488–499, doi: 10.1016/j.asr.2011.03.040.
- Liperovsky V. A., Pokhotelov O. A., Liperovskaya E. V., Parrot M., Meister C.-V., Alimov O. A., 2000: Modification of sporadic E-layers caused by seismic activity. *Surv. Geophys.*, **21**, 5-6, 449–486, doi: 10.1023/A:1006711603561.
- Liu J. Y., Chang F. Y., Chen Y. I., Chang L. C., Wen Y. C., Wu T. Y., Chao C. K., 2023: Pre-earthquake ionospheric anomalies and ionospheric storms observed by FORMOSAT-5/AIP and GIM TEC. *Surv. Geophys.*, doi: 10.1007/s10712-023-09807-7.
- Liu J. Y., Chen Y. I., Chuo Y. J., Chen C. S., 2006: A statistical investigation of preearthquake ionospheric anomaly. *J. Geophys. Res. Space Phys.*, **111**, A5, A05304, doi: 10.1029/2005JA011333.
- Liu J. Y., Chen C. H., Chen Y. I., Yang W. H., Oyama K. I., Kuo K. W., 2010: A statistical study of ionospheric earthquake precursors monitored by using equatorial ionization anomaly of GPS TEC in Taiwan during 2001–2007. *J. Asian Earth Sci.*, **39**, 1-2, 76–80, doi: 10.1016/j.jseaes.2010.02.012.
- Liu J. Y., Chuo Y. J., Shan S. J., Tsai Y. B., Chen Y. I., Pulnits S. A., Yu S. B., 2004: Pre-earthquake ionospheric anomalies registered by continuous GPS TEC measurements. *Ann. Geophys.*, **22**, 5, 1585–1593, doi: 10.5194/angeo-22-1585-2004.
- Mallat S., 1999: A wavelet tour of signal processing. Academic Press, Elsevier, 577 p.
- Molchanov O. A., Hayakawa M., 2008: Seismo-electromagnetics and related phenomena: History and latest results. Terrapub, Tokyo, 189 p.
- Molchanov O., Fedorov E., Schekotov A., Gordeev E., Chebrov V., Surkov V., Rozhnoi A., Andreevsky S., Iudin D., Yunga S., Lutikov A., Hayakawa M., Biagi P. F., 2004: Lithosphere-atmosphere-ionosphere coupling as governing mechanism for preseismic short-term events in atmosphere and ionosphere. *Nat. Hazards Earth Syst. Sci.*, **4**, 5-6, 757–767, doi: 10.5194/nhess-4-757-2004.
- Namgaladze A. A., Klimenko M. V., Klimenko V. V., Zakharenkova I. E., 2009: Physical mechanism and mathematical modeling of earthquake ionospheric precursors registered in total electron content. *Geomagn. Aeron.*, **49**, 2, 252–262, doi: 10.1134/S0016793209020169.
- Pulnits S. A., Ouzounov D., Karelin A. V., Boyarchuk K. A., Pokhmelnikh L. A., 2006: The physical nature of thermal anomalies observed before strong earthquakes. *Phys. Chem. Earth, Parts A/B/C*, **31**, 4-9, 143–153, doi: 10.1016/j.pce.2006.02.042.

- Pulinets S., Ouzounov D., 2011: Lithosphere–Atmosphere–Ionosphere Coupling (LAIC) model – An unified concept for earthquake precursors validation. *J. Asian Earth Sci.*, **41**, 4–5, 371–382, doi: 10.1016/j.jseaes.2010.03.005.
- Rama Rao P. V. S., Niranjana K., Prasad D. S. V. V. D., Gopi Krishna S., Uma G., 2006: On the validity of the ionospheric pierce point (IPP) altitude of 350 km in the Indian equatorial and low-latitude sector. *Ann. Geophys.*, **24**, 8, 2159–2168, doi: 10.5194/angeo-24-2159-2006.
- Rikitake T., 1968: Earthquake prediction. *Earth-Sci. Rev.*, **4**, 245–282, doi: 10.1016/0012-8252(68)90154-2.
- Seemala G. K., 2011: GPS-TEC analysis application. Technical document, available online: <http://seemala.blogspot.com>.
- Shah M., Jin S., 2015: Statistical characteristics of seismo-ionospheric GPS TEC disturbances prior to global $M_w \geq 5.0$ earthquakes (1998–2014). *J. Geodyn.*, **92**, 42–49, doi: 10.1016/j.jog.2015.10.002.
- Sharma G., Champati ray P. K., Mohanty S., Kannaujiya S., 2017: Ionospheric TEC modelling for earthquakes precursors from GNSS data. *Quat. Int.*, **462**, 65–74, doi: 10.1016/j.quaint.2017.05.007.
- Singh R. P., Dey S., Bhoi S., Sun D., Cervone G., Kafatos M., 2006: Anomalous increase of chlorophyll concentrations associated with earthquakes. *Adv. Space Res.*, **37**, 4, 671–680, doi: 10.1016/j.asr.2005.07.053.
- Tariq M. A., Shah M., Hernández-Pajares M., Iqbal T., 2019: Pre-earthquake ionospheric anomalies before three major earthquakes by GPS-TEC and GIM-TEC data during 2015–2017. *Adv. Space Res.*, **63**, 7, 2088–2099, doi: 10.1016/j.asr.2018.12.028.
- Troyan V. N., Hayakawa M., 2002: Seismo electromagnetics: lithosphere–atmosphere–ionosphere coupling. In: Hayakawa M., Molchanov O. A. (Eds.): *Seismo Electromagnetics: Lithosphere–Atmosphere–Ionosphere Coupling*. Terra Scientific Publishing, Tokyo, 215–221.
- Ulukavak M., Yalçınkaya M., Kayıkçı E. T., Öztürk S., Kandemir R., Karlı H., 2020: Analysis of ionospheric TEC anomalies for global earthquakes during 2000–2019 with respect to earthquake magnitude ($M_w \geq 6.0$). *J. Geodyn.*, **135**, 101721, doi: 10.1016/j.jog.2020.101721.
- Uyeda S., Nagao T., Kamogawa M., 2009: Short-term earthquake prediction: Current status of seismo-electromagnetics. *Tectonophysics*, **470**, 3–4, 205–213, doi: 10.1016/j.tecto.2008.07.019.
- Wang X., Sun Q., Eastes R., Reinisch B., Valladares C. E., 2008: Short-term relationship of total electron content with geomagnetic activity in equatorial regions. *J. Geophys. Res. Space Phys.*, **113**, A11, doi: 10.1029/2007JA012960.
- Yadav K. S., Karia S. P., Pathak K. N., 2016a: Removal of solar radiation effect based on nonlinear data processing technique for Seismo-Ionospheric Anomaly before few earthquakes. *Geomatics, Nat. Hazards Risk*, **7**, 3, 1147–1161, doi: 10.1080/19475705.2015.1021864.
- Yadav K., Karia S. P., Pathak K. N., 2016b: Anomalous variation in GPS TEC, land and ocean parameters prior to 3 earthquakes. *Acta Geophys.*, **64**, 1, 43–60, doi: 10.1515/acgeo-2015-0057.

- Yadav K. S., Pathak J. S., 2018: Anomalous variation in GPS based Total Electron Content (TEC), prior to six (6) earthquakes in 2016. *MAUSAM*, **69**, 3, 419–426, doi: [10.54302/mausam.v69i3.332](https://doi.org/10.54302/mausam.v69i3.332).
- Yadav K. S., Vadrnathani R. B., Goswami K. R., Patel P. M., 2023: Anomalous variations in ionosphere TEC before the earthquakes of 2021 in the different parts of the globe. *Trends Sci.*, **20**, 8, 5169, doi: [10.48048/tis.2023.5169](https://doi.org/10.48048/tis.2023.5169).
- Zhu F., Jiang Y., 2020: Investigation of GIM-TEC disturbances before $M \geq 6.0$ inland earthquakes during 2003–2017. *Sci. Rep.*, **10**, 18038, doi: [10.1038/s41598-020-74995-w](https://doi.org/10.1038/s41598-020-74995-w).